Effect of Zinc Binding on the Structure and Stability of Fibrolase, a Fibrinolytic Protein from Snake Venom

Denise Pretzer,[1] Brenda Schulteis,[2] David G. Vander Velde,[3] Christopher D. Smith,[4] James W. Mitchell,[5] and Mark C. Manning[6,7]

Received August 20, 1991; accepted January 29, 1992

Fibrolase is a metalloprotease with potential use as a fibrinolytic agent. Loss of the intrinsic zinc atom leads to a rapid decrease in enzymatic activity. Circular dichroism measurements indicate that there is a partial unfolding of an α-helical section of the protein concomitant with the loss of zinc. Removal of zinc can be affected by elevated temperatures, acidic pH values, and addition of chelating agents. At low molar concentrations, both ethylenediaminetetraacetic acid (EDTA) and dithiothreitol (DTT) were found to remove zinc efficiently. Analysis of the sequence of fibrolase identified a segment which possessed a high degree of homology with the metal binding site of other zinc proteases, such as thermolysin and the collagenases. However, the putative zinc binding site in fibrolase lacks the additional glutamate ligand found in thermolysin and subtilisin. This sequence is also predicted to adopt an α-helical conformation. Together, these data indicate that there is a well-defined metal binding site in fibrolase and that metal binding is the most important factor governing the stability of this protein.

KEY WORDS: fibrolase; metalloprotease; zinc binding; enzyme; sequence; protein structure.

INTRODUCTION

Protein therapeutic agents have become an integral part of the pharmaceutical industry, especially with the advances in recombinant DNA technology. As a result, it is imperative to develop integrated approaches for assessing the stability of these materials. Incorporating spectroscopic, chromatographic, and biochemical methods into a concerted preformulation study appears to provide the most accurate description of the stability of protein pharmaceuticals.

Originally isolated from snake venom, fibrolase is a protein which possesses potential for use in thrombolytic therapy. Fibrolase is a small protease, containing only 203 amino acids in known sequence (1), shown in Fig. 1, and acts on fibrin directly. The enzymatic activity of fibrolase has been shown to be dependent on the presence of zinc (2). Fibrolase has a p*I* of approximately 6.7 (3) and has been classified a metalloprotease due to its zinc requirement (4). In addition, it has been shown to possess an appreciable α-helical content and that the overall globular structure is quite thermally stable (5). Isoenzymes of fibrolase are thought to exist due to evidence of sequence heterogeneity from the natural source and observation of multiple bands on isoelectric focusing (IEF) gels of relatively pure fibrolase preparations (4).

The effects of temperature and pH on the stability of fibrolase in aqueous solution have been studied in detail (5). In this study, the role of zinc in stabilizing fibrolase is examined and a putative zinc binding site is proposed. Also, a general description of the secondary structural composition of fibrolase is developed based upon sequence analysis and circular dichroism (CD) spectroscopy.

MATERIALS AND METHODS

Fibrolase may be obtained from the venom of the southern copperhead snake by a multistep fractionation procedure and was purified according to the procedure of Ahmed *et al.* (2).

Proteolytic Activity Assays

The proteolytic activity of fibrolase was assessed using two substrates: the oxidized B chain of insulin and azocasein.

Insulin B-Chain Substrate. The proteolytic activity assay using the oxidized B chain of insulin has been described previously (3,5). The activity of fibrolase versus insulin B chain was determined by incubating fibrolase with the oxidized form of insulin B chain at 37°C. The molar excess of substrate was approximately 250 to 1500. After incubation, the reaction was quenched by addition of EDTA. The remaining insulin B chain was quantitated by HPLC. To determine the proteolytic activity in samples, assay results were compared to results obtained concurrently for fibrolase standards of known activity.

Azocasein Substrate. Azocasein was synthesized by diazotization of casein as described previously (6). Fibrolase was incubated at 37°C with azocasein. The molar excess of substrate ranged from about 6 to 60. The reaction was quenched by the addition of perchloric acid. Following centrifugation, acid-soluble azopeptides, resulting from the action of fibrolase on azocasein, were quantitated by absorbance at 390 nm. Proteolytic activity in samples was determined by comparison to standards from a fibrolase lot of known activity, assayed concurrently.

Proteolytic activity of fibrolase was found to be correlated with bioactivity as demonstrated using *in vitro* clot lysis or fibrin plate assays. Fibrolase reproducibly demonstrated activity in these assays, however, the enzyme activity assays were better suited for routine analyses.

Spectroscopic Methods

All CD spectra were obtained on an Aviv 60DS spectrophotometer equipped with a Lauda temperature bath, using jacketed quartz cells (Hellma) with pathlengths of 0.5–5.0 mm. During studies at elevated temperatures, the sample was equilibrated at each temperature for about 10 min, and

[1] Merck, Sharp, and Dohme Research Laboratories, West Point, Pennsylvania 19486.
[2] Marion Merrell Dow Research Institute, Kansas City, Missouri 64134.
[3] NMR Laboratory, University of Kansas, Lawrence, Kansas 66045.
[4] Department of Pharmaceutical Chemistry, University of Kansas, Lawrence, Kansas 66045.
[5] OREAD Laboratories, Inc., Lawrence, Kansas 66047.
[6] School of Pharmacy, Campus Box C238, University of Colorado Health Sciences Center, 4200 East 8th Street, Denver, Colorado 80262.
[7] To whom correspondence should be addressed.

0724-8741/92/0700-0870$06.50/0

Gln Gln Arg Phe Pro Gln Arg Tyr Val Gln Leu Val Ile Val Ala Asp His Arg
Met Asn Thr Lys Tyr Asn Gly Asp Ser Asp Lys Ile Arg Gln Trp Val His Gln
Ile Val Asn Thr Ile Asn Glu Ile Tyr Arg Pro Leu Asn Ile Gln Phe Thr Leu
Val Gly Leu Glu Ile Trp Ser Asn Gln Asp Leu Ile Thr Val Thr Ser Val Ser
His Asp Thr Leu Ala Ser Phe Gly Asn Trp Arg Glu Thr Asp Leu Leu Arg Arg
Gln Arg His Asp Asn Ala Gln Leu Leu Thr Ala Ile Asp Phe Asp Gly Asp Thr
Val Gly Leu Ala Tyr Val Gly Gly Met Cys Gln Leu Lys His Ser Thr Gly Val
Ile Gln Asp His Ser Ala Ile Asn Leu Leu Val Ala Leu Thr Met Ala His Glu
Leu Gly His Asn Leu Gly Met Asn His Asp Gly Asn Gln Cys His Cys Gly Ala
Asn Ser Cys Val Met Ala Ala Met Leu Ser Asp Gln Pro Ser Lys Leu Phe Ser
Asp Cys Ser Lys Lys Asp Tyr Gln Thr Phe Leu Thr Val Asn Asn Pro Gln Cys
Ile Leu Asn Lys Pro

Fig. 1. Sequence of native fibrolase.

the temperature of the water bath was recorded as the sample temperature. Maximum deviation of the sample and bath temperatures was estimated to be 2°C. Protein concentrations ranged from 0.060 to 0.800 mg/ml. All spectra were smoothed and baseline-corrected prior to plotting. A mean residue weight of 113.2 was employed in the calculation of molar ellipticity values.

Electrophoresis and Protein Quantitation

The purity of fibrolase was monitored using various electrophoretic techniques. Determinations of the protein concentration was accomplished by standard chemical methods described below.

Gel Electrophoresis. All gels were run on the Pharmacia Phast (TM) system, according to the manufacturer's instructions. Prepared gels were obtained from Pharmacia. Sodium dodecyl sulfate–polyacrylamide gel electrophoresis (SDS–PAGE) and native gels were run on 8–25% gradients. IEF gels were done covering the pH range of 3 to 9. For all gels, bands were detected by staining with Coomassie blue. Samples analyzed by SDS–PAGE contained approximately 0.13 *M* (3.7%) SDS. Reduced samples were prepared by the addition of 0.66 *M* (5%) β-mercaptoethanol and heating at 95°C for 5 to 10 min. Samples for native gels and IEF gels were applied without dilution or diluted with water or 10 m*M* Tris buffer (pH 8).

Protein Quantitation. Protein concentrations were determined using the Pierce microBCA kit. The assay is based upon the reaction of protein with Cu^{2+} to form Cu^{+}, which complexes with bicinchoninic acid (BCA), forming a colored product whose intensity at 562 nm is related to the protein concentration. The extinction coefficient of fibrolase at 280 nm was determined based on measurements of several lots in Hepes buffer (pH 7.5). The average was 1.05 for a 1 mg/ml solution.

Sequence Analysis

Sequence homology analyses were conducted using EuGene software searching the PIR sequence data banks. Hydrophobic moments were calculated using the method of Eisenberg *et al.* (7,8).

RESULTS

Effect of EDTA on the Stability of Fibrolase

The effect of addition of EDTA on the activity and conformation of fibrolase was of interest due to the classification of fibrolase as a zinc metalloprotein (2–5). Other investigators had previously observed inhibition of azocaseinolytic activity of fibrolase by EDTA, and, in fact, these studies contributed to the characterization of fibrolase as a metalloprotein (2,4). It was of interest to investigate what concentrations of EDTA are required to affect fibrolase activity and what other changes (e.g., structural) are caused by EDTA addition.

The effect of EDTA on proteolytic activity of fibrolase is dependent on the EDTA concentration added (see Table I). Partial inhibition was observed for EDTA concentrations as low as 0.1 m*M* (the concentration of fibrolase was ~100 μg/ml). Complete inhibition occurred at 0.9 m*M* EDTA for activity versus the insulin B chain. Further increases in EDTA concentration had no effect. Activity for the insulin B chain was inhibited to a greater extent than was the azocaseinolytic activity. About half of the azocaseinolytic activity remained in the presence of 1 m*M* EDTA. A higher EDTA concentration, 5 m*M*, was required for essentially complete (98%) inhibition of azocaseinolytic activity. The time course for the inactivation of fibrolase by EDTA was rapid (Fig. 2). Inhibition was complete at the first measurable time point for 6 and 20 m*M* EDTA using insulin B chain as the substrate and remained complete over 1 hr. The time course of inhibition was not followed for other EDTA concentrations.

While submillimolar concentrations of EDTA (<1 m*M*) resulted in a partial loss of activity versus insulin B chain and azocasein, changes in CD spectra were also noted at these EDTA concentrations (Fig. 3). These amounts of EDTA represent only a 10- to 40-fold molar excess of EDTA compared to fibrolase. At 0.1 m*M* EDTA, the molar excess of EDTA over fibrolase was only about 25 for studies examining the effect on activity and 10–15 in the case of the CD work and was sufficient to observe significant changes in structure and

Table I. Proteolytic Activity of Fibrolase in the Presence of EDTA

[EDTA] (m*M*)	% activity remaining relative to control[a]	
	vs insulin B chain	vs azocasein
0.1	51.4 (9.3)	55.2 (12.0)
0.2	51.8 (15.8)	50.1 (12.5)
0.5	32.7 (6.9)	49.6 (14.5)
0.9	0	nd[b]
1.0	nd	42.1 (12.5)
2.0	nd	22.6 (3.8)
5.0	nd	2.3 (0.1)
6.0	0	nd
20.0	0	nd

[a] No EDTA was added to the control samples. Initial fibrolase concentration was ~100 μg/ml. Numbers reported are the means of at least three determinations, with standard deviations given in parentheses.

[b] Not determined.

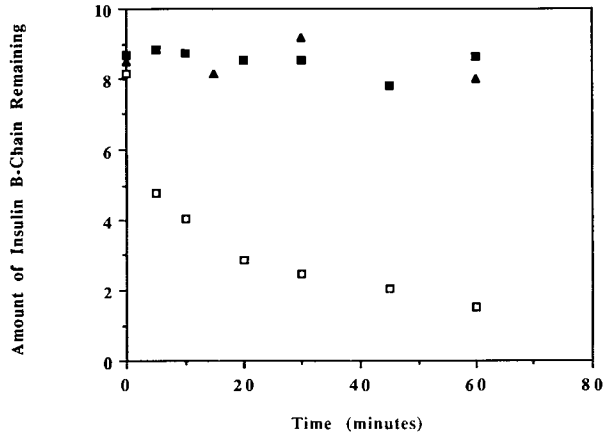

Fig. 2. Time course of EDTA inhibition of fibrolase proteolytic activity. The substrate was insulin B chain and the amount remaining was determined by HPLC and represents peak area ($\times 10^{-2}$). Decreasing peak area indicates activity and the assay variability was typically ~5%. Activity was monitored in samples containing 0 m*M* EDTA (□), 6 m*M* EDTA (▲), and 20 m*M* EDTA (■).

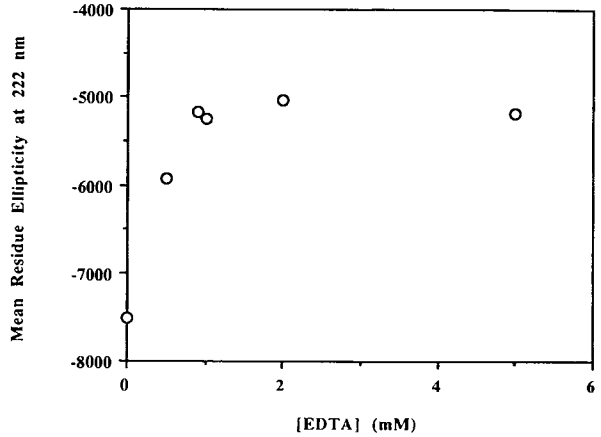

Fig. 4. Dependence of the mean residue ellipticity of fibrolase at 222 nm (280 μg/ml) on EDTA concentration.

activity. The low concentration and molar excess of EDTA necessary to induce activity and structural changes in fibrolase indicated that the zinc ion is quite loosely bound to the protein. A plot of EDTA concentration versus mean residue ellipticity at 222 nm (Fig. 4) indicates that the zinc is completely removed at concentrations above 1.0 m*M*. Further increases in EDTA concentration had no effect. Similar amounts of EDTA caused complete inhibition of proteolytic activity (see above).

Other chelators were also found to be effective at removing zinc from fibrolase. The addition of dithiothreitol (DTT) to a solution of fibrolase led to changes in the CD spectra which were similar to those produced by EDTA or upon lowering the pH (Fig. 5). While DTT is usually considered a reducing agent, it is also known to be a chelating agent (9).

Changes observed upon EDTA addition to fibrolase were detected by gel electrophoresis as well (Fig. 6). Native gels displayed a downward shift of the fibrolase bands in the presence of EDTA (>1 m*M*). With samples not containing EDTA, several low molecular weight bands were observed in addition to the main band of fibrolase. Multiple bands were observed on IEF gels (Fig. 6), the darkest of which was centered at a p*I* of approximately 6.7. Double bands of lighter intensity were seen both above and below the main band, indicative of the existence of isozymes of fibrolase. Upon addition of EDTA, the band above the main band diminished significantly in intensity. Taken in conjunction with the CD results, these observed changes indicate a change in the structure of fibrolase upon zinc removal.

Attempts to remove zinc so that other metals might be reconstituted into fibrolase failed. Dialysis against other metal salts, such as cobalt(II) salts, in either the presence or the absence of EDTA, were ineffective in substituting cobalt for zinc, although dialysis against cobalt-containing solutions has lead to metal exchange for other zinc-containing enzymes found in snake venom (10). Removal of the zinc atom from fibrolase typically leads to rapid aggregation and precipitation. The addition of zinc chloride or any other salts produced minimal renaturation (see Fig. 7), with most of the fibrolase precipitating. This was especially true at high protein concentrations (1–5 mg/ml). The refolded form (Fig. 7) has a significantly higher β-sheet content than native fibro-

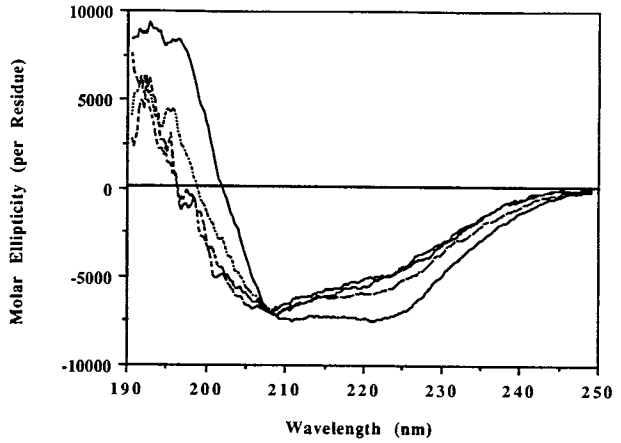

Fig. 3. Far-UV CD spectra of fibrolase (280 μg/ml) in 10 m*M* phosphate buffer containing 0.0 m*M* (——), 0.5 m*M* (····), 0.9 m*M* (---), and 2.0 m*M* (– –) EDTA. The pathlength was 1.0 mm.

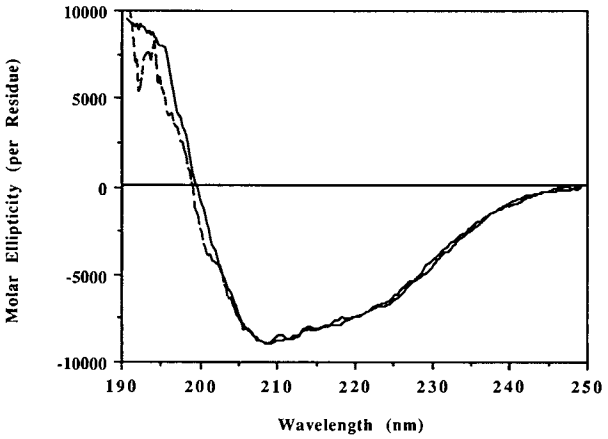

Fig. 5. Far-UV CD spectrum of fibrolase (414 μg/ml) at pH 3 (——) and of fibrolase (239 μg/ml) at pH 8 with 10 m*M* DTT added (– –). The pathlength was 0.5 mm for the pH 3 sample and 1.0 mm for the DTT sample.

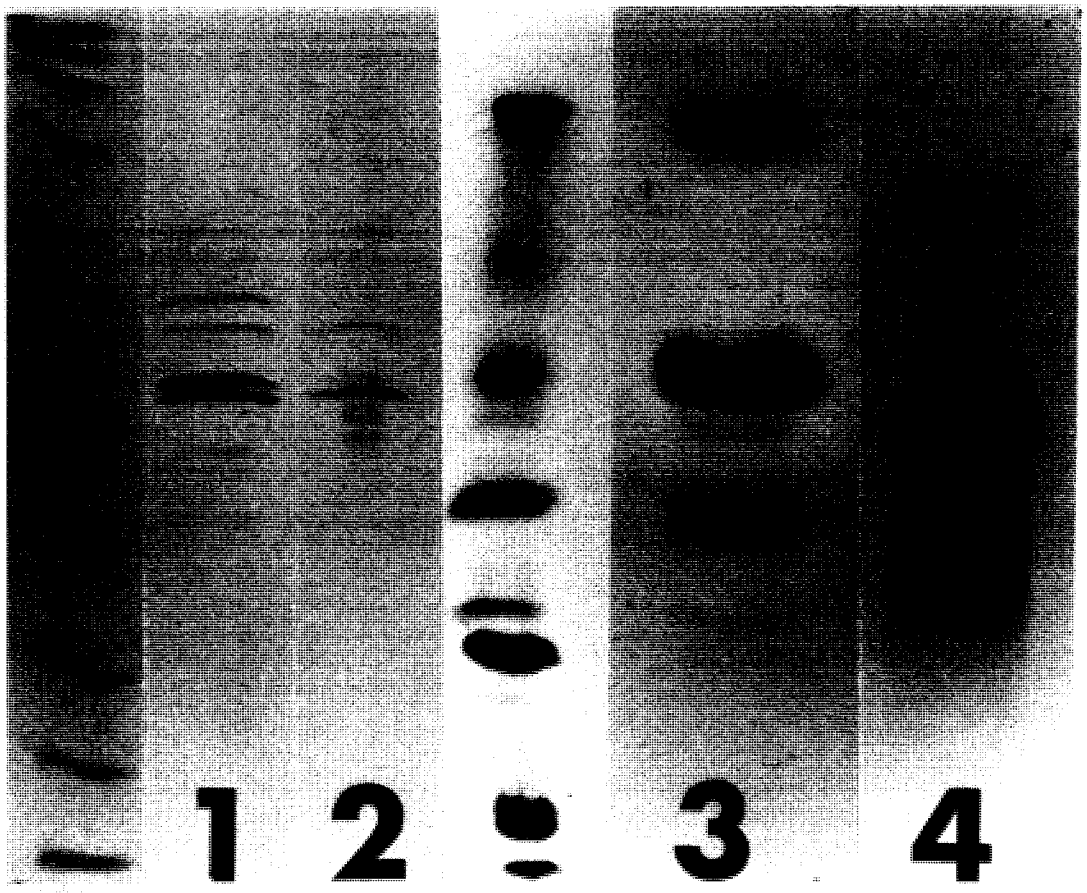

Fig. 6. Gels of fibrolase before and after EDTA treatment. Lane 1: Isoelectric focusing (IEF) gel of fibrolase without EDTA. Lane 2: IEF gel of fibrolase with the addition of EDTA. Lane 3: SDS–PAGE gel of fibrolase without EDTA. Lane 4: SDS–PAGE gel of fibrolase with the addition of EDTA. The lane to the left of Lane 1 shows the pH markers for the IEF gel. The lane between Lane 2 and Lane 3 shows the molecular weight markers for the SDS–PAGE gel.

lase (Fig. 7), as seen by a more distinct minimum near 217 nm. In contrast, native fibrolase displays two negative bands, at 222 and 207 nm (Fig. 3), indicative of a significant α-helix content.

Sequence Analysis of the Metal Binding Site

While the exact location of the intrinsic zinc atom is not known for fibrolase, the metal binding site has been identified for many zinc-containing enzymes (11,12), primarily through X-ray crystallography. The sequence of fibrolase (1) was compared to those of other metalloproteases and it was found that the zinc binding sites of thermolysin and subtilisin display a high degree of homology with a segment of fibrolase (Table II). However, further analysis showed that the final glutamate ligand, located at position 166 of thermolysin and subtilisin, appears to be missing in fibrolase (Table II). However, there is another class of zinc proteases which possesses an even higher degree of homology with fibrolase. These are the collagenases. The AHELGH core sequence is identical to the central metal binding site in all of the collagenases that have been sequenced to date. In addition, there is a conserved sequence in the C-terminal portion of collagenases which is reproduced in fibrolase as well (Table II). Overall, this appears to substantiate that there is a well-defined zinc binding site in fibrolase and that it is similar to that found in other zinc-containing enzymes. Upon addition of EDTA, the zinc atom is irreversibly removed from fibrolase. Concomitant with the loss in activity is a marked change in the far-UV CD spectrum. Secondary structure analysis suggests that more than half of the α-helix content is lost in this transition. The α-helix content drops from ~24 to ~10%, based upon deconvolutions using the data base of Chang *et al.* (13), suggesting that the metal binding site

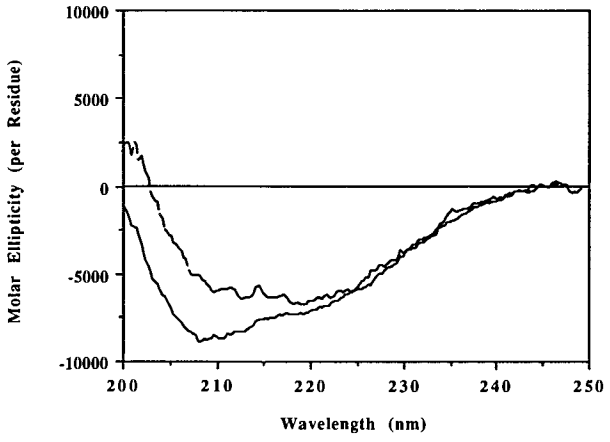

Fig. 7. Far-UV CD spectra of fibrolase (73 μg/ml) at pH 2 (——) and of fibrolase at pH 2 plus 860 m*M* NaCl (– –). The pathlength was 1.0 mm.

Table II. Sequence Comparison for Proposed Fibrolase Zinc Binding Site and Other Zinc Proteases

Fibrolase 140–150	T	M	A	H	E	L	G	H	N	L	G
Hemorrhagic toxin d (*Crotalus atrox*) 140–150	T	M	A	H	E	L	G	H	N	L	G
Thermolysin 139–149	V	V	A	H	E	L	T	H	A	V	T
E. coli aminopeptidase N 139–149	V	I	G	H	E	Y	F	H	N	W	T
Subtilisin 140–150	V	T	A	H	E	M	T	H	G	V	T
Human collegenase 215–225	V	A	A	H	E	L	G	H	S	L	G
Rabbit collegenase 215–225	V	A	A	H	E	L	G	H	S	L	G
Human collagenase IV 215–225	V	A	A	H	E	F	G	H	A	L	G
Human stromelysin-2 214–224	V	A	A	H	E	L	G	H	S	L	G
Human metalloproteinase-1 211–221	A	A	T	H	E	L	G	H	S	L	G
Human metalloproteinase-3 215–225	V	A	A	H	E	I	G	H	S	L	G
Fibrolase 162–170	A	N	S	C	V	M	A	A	M		
Hemorrhagic toxin d (*Crotalus atrox*) 140–150	A	S	L	C	I	M	R	P	G		
Thermolysin 162–170	G	A	I	N	E	A	I	S	D		
E. coli aminopeptidase N 162–170	L	S	L	K	E	G	L	T	V		
Subtilisin 162–170	G	A	L	N	E	S	F	S	D		

Glu^{166} is the third ligand (after the two histidines) in thermolysin and subtilisin. There is no such ligand in fibrolase. There seems to be a better homology with collagenases and other snake toxins, not only in the metal binding site but elsewhere in the C terminus.

Fibrolase 175–185	P	S	K	L	F	S	D	C	S
Hemorrhagic toxin d (*Crotalus atrox*) 140–150	R	S	Y	E	F	S	D	D	S
Human collegenase 238–246	P	S	Y	T	F	S	G	D	V
Rabbit collegenase 238–246	P	N	Y	M	F	S	G	D	V
Human collagenase IV 238–246	P	M	Y	R	F	T	E	G	P
Human stromelysin-2 238–246	P	L	Y	N	S	F	T	E	L
Human metalloproteinase-3 239–247	P	L	Y	H	S	L	T	D	L

adopts an α-helical conformation. These results are consistent with the secondary structure analysis described below. No consensus sequence is found in fibrolase which corresponds to a "cysteine switch" (14).

Secondary Structure Analysis of Fibrolase

Identification of α-helical segments in fibrolase was accomplished using secondary structure prediction methods. The primary scheme used was that of Cid *et al.* (15), which employs hydrophobicity and solvent accessibility as indicators of secondary structure types. For example, a hydrophobicity plot of residues 20–50 in fibrolase (Fig. 8) shows a number of residues having values which alternate in pairs above and below the average. This is indicative of an exposed α-helical structure. This helix, covering residues 30 through 49, accounts for approximately 10% of the total residues. Figure 8 also indicates that residues 26–29, being hydrophilic in nature, are involved in a β turn leading into the α helix. The second significant α helix, which includes the histidines involved in the putative metal binding site, is predicted to extend from residue 140 to residue 152. A final helical segment is predicted to occur at residues 168–175. The pattern of alternating pairs of residues is difficult to detect in the hydrophobicity plot for residues 130–160 (Fig. 9) but is easier to identify in the solvent accessibility plot (Fig. 10). This is due mostly to the lack of correlation between hydrophobicity and solvent accessibility for His and Gly, both of which are present in high numbers in this helical segment. Other algorithms were used to confirm the presence of an α-helical structure in this region. Chou–Fasman parameters (16) gave a decided preference to the α helix versus β structure (P = 1.08 vs 0.95), while the method of Garnier *et al.* (17) identified this segment as being one of the strongest in α-helical character (see Table III).

The method of Garnier *et al.* (17), while predicting the two C-terminal α helices, places two smaller helices at residues 15–19 and 84–91 in place of the α helix predicted by the method of Cid *et al.* (15) at residues 30–49. Each of the methods (Cid *et al.* and Garnier *et al.*) indicate a total helix content of ~25%, in close agreement with the CD analysis. A more detailed comparison is given in Table III. While there are some differences in the positioning of certain secondary structures, there is some agreement. For example, the metal binding site is predicted to be helical by both methods. Other large secondary structures such as a long β strand (residues 109–122) are similarly predicted. Agreement is also

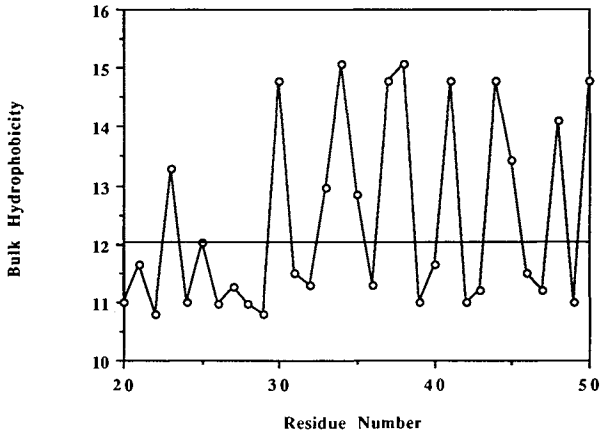

Fig. 8. Hydrophobicity plot for residues 20–50 in fibrolase using the scale of Cid *et al.* (15).

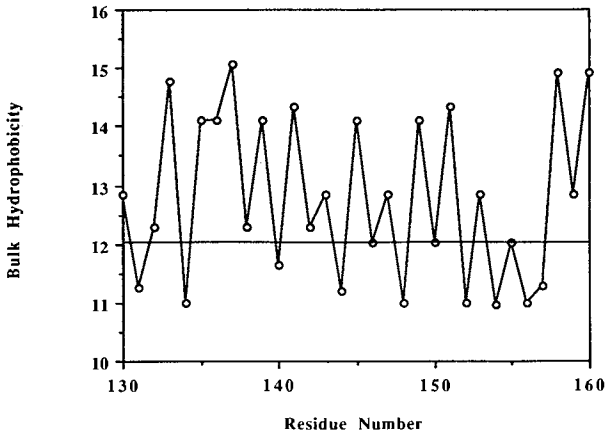

Fig. 9. Hydrophobicity plot for residues 130–160 of native fibrolase using the scale of Cid *et al.* (15).

found for certain β turns, such as at positions 61–65, 152–157, and 182–186.

Analysis of the zinc binding site indicated that the α helix possesses some amphiphilic character. The hydrophobic moment was calculated to be 0.11 for this sequence. A helix wheel diagram (Fig. 11) indicates the existence of a hydrophobic face on the metal binding helix.

DISCUSSION

The addition of chelating agents, such as EDTA and DTT, has a profound effect on both the structure and the activity of fibrolase. While EDTA treatment does diminish the proteolytic activity of fibrolase, it does not equally affect it for all substrates. The reason for the difference in effective inhibitory concentrations of EDTA might be related to the difference in molecular size of the two substrates. The molecular weight of insulin B chain is about 3800, while that of azocasein is about 25,000. Because of the size difference, the substrates might be subject to different constraints around the active site of fibrolase. The data indicated that the active-site constraints, or importance of metal binding, might be greater for the insulin B chain, since this activity was inhibited at lower EDTA concentrations. Conversely, these observations are in contrast to previous studies which suggested that azocaseinolytic activity was lost more readily than was activity for the insulin B chain at pH extremes (pH <4) and after extended storage at room temperature. Most likely, this is due to additional structural changes which occur upon exposing fibrolase to severe conditions such as prolonged storage or acidic pH.

Structural changes, as detected by CD, correlate with the observed activity changes. At submillimolar EDTA concentrations, structural changes were evident by CD as indi-

Table III. Comparison of the Positioning of Secondary Structural Features in Native Fibrolase by the Methods of Cid *et al.* (15) and Garnier *et al.* (17)

Cid *et al.* (15)	Garnier *et al.* (17)
α helix	
29–47	15–19
65–75 (weak)	84–91
94–101	
140–153	132–147
165–173	164–175
β sheet	
10–16	1–5, 7–13
	29–46
48–59	49–58
	65–77
101–106	98–103
109–122	109–120
	125–132
	187–193
195–200	198–202
β turns	
1–3, 4–6	
25–29	
61–65	62–64
84–86	
89–92	92–94
	105–107
122–125	
154–157	152–156
	159–162
174–177	
182–186	182–185
193–196	

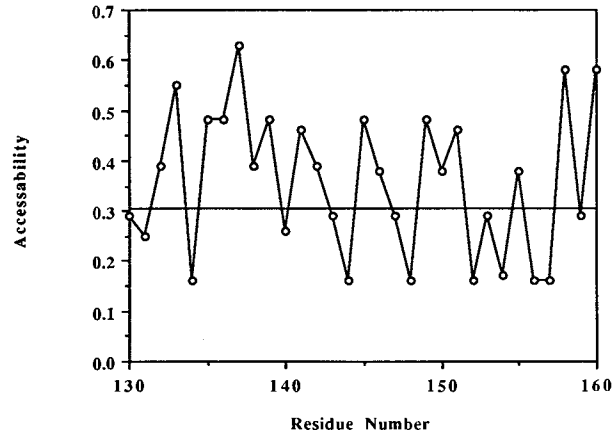

Fig. 10. Solvent accessibility plot for fibrolase (residues 130–160) using the scale of Cid *et al.* (15).

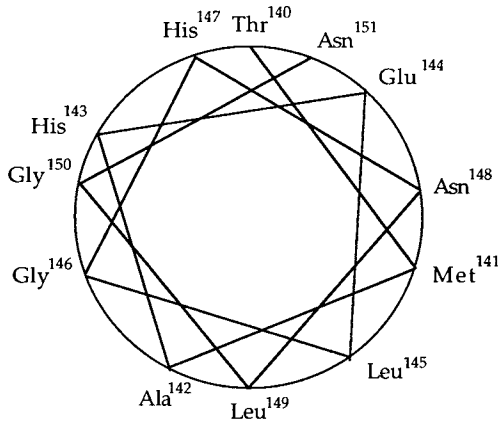

Fig. 11. Helix wheel diagram for the putative zinc binding site in fibrolase.

cated by decreasing elliptical intensity at 222 nm (Fig. 4). At EDTA concentrations greater than or equal to 0.9 m*M* (fibrolase concentration, ~100 μg/ml), the spectral changes observed by CD appeared to be complete. Similar concentrations of EDTA have been found to inactivate other zinc proteases, such as the hemorrhagic toxins found in snake venoms (18–20). Deconvolution of the CD data indicated that nearly all of the changes could be attributed to a loss of α-helical structure. A decrease from 24 to 10% was determined using the basis sets of Chang *et al.* (13). The addition of EDTA and other chelating agents has been found to lower the helix content markedly in other zinc proteases (19,20). For hemorrhagic toxin e, the amount of α helix decreased from 23 to 7% upon EDTA treatment as determined by CD spectroscopy (19). Similar changes in fibrolase were noted upon lowering the pH to below 4 or upon increasing the temperature to above 45°C (5), although some minor differences between these CD spectra can be seen. All of the data are consistent with the loss of the essential zinc ion. A decrease in pH would lead to protonation of the central His residues, thereby diminishing their liganding capability. Moderate increases in temperature also disrupt the metal binding. Recent studies have shown that metal binding can significantly stabilize isolated α helices (21–23).

Changes similar to those observed upon addition of EDTA were also noted upon addition of DTT (Fig. 5). While DTT is a well-known reducing agent, it is also a good chelating agent (9). The similarity of the CD spectrum of DTT-treated fibrolase with those obtained upon EDTA addition (Figs. 4 and 5) suggests strongly that DTT acts to remove the zinc from fibrolase rapidly and easily. Complete retention of the near-UV CD spectrum following DTT and EDTA treatment (results not shown) indicates that the disulfides have not been disrupted and that DTT is acting directly on the metal center.

Attempts at reconstituting zinc into fibrolase after DTT treatment failed. With both EDTA- and DTT-treated fibrolase, loss of the zinc leads to an unfolded structure which is much more susceptible to aggregation and precipitation, making reconstitution very difficult. Dialysis experiments were constructed to replace zinc with cobalt, which has been done for other proteins (9,24,25). These led to little or no native fibrolase remaining in solution. While the zinc appears to be loosely bound, it does not appear to be in facile exchange with zinc free in solution. Lowering the pH below 4 also leads to loss of zinc, probably via protonation of the His residues, thereby reducing the affinity to bind metals (5). The low-pH form appears by CD to be very similar in structure to the EDTA-treated form (Fig. 6). Acid- and base-induced denatured proteins can often be renatured to compact forms, resembling the so-called "molten globule" state upon the addition of large amounts of salt (26,27). While the addition of excess $ZnCl_2$ leads to precipitation of fibrolase at high concentrations (>1 mg/ml), at concentrations lower than 0.1 mg/ml, some fibrolase can be refolded (Fig. 7). The increase in ellipticity near 217 nm and the loss of two distinct negative features in this region suggests a loss of α-helical structure and an increase in β-sheet content. Other salt-renatured proteins have also shown increased amounts of β sheet (28).

The electrophoresis data showed that not only is the presence of the metal ion critical for proteolytic activity, but also it is important to the structure of the protein. Migration of fibrolase on native gels was altered upon removal of zinc by EDTA. While this does not demonstrate the existence of a single zinc binding site, it does suggest that zinc ions bind to fibrolase and affect its structural properties. These results are consistent with the CD measurements and the enzymatic activity assays.

Heterogeneity in the sequence of fibrolase was indicated by IEF electrophoresis. Appearance of bands at both lower and higher p*I* values than the main band was observed. The addition of EDTA led to a significant loss of one of the minor components, possibly due to weaker zinc binding in that isozyme. However, the electrophoretic properties of all fibrolase species were affected by the addition of chelating agents.

Sequence analysis divulged that a portion of fibrolase is highly homologous to the metal binding regions of other zinc proteases, such as thermolysin, subtilisin, and the collagenases. Some differences can be seen. Fibrolase appears to lack the final Glu ligand which occurs in both thermolysin and subtilisin. This may account for a relatively low binding affinity for the zinc in fibrolase. There is a much higher degree of homology with members of the collagenase family (Table II). In fact, the central sequence of fibrolase is identical with those of the collagenases except for substitutions of Asn^{148} with either Ser or Ala. Another portion of the sequence which displays some homology is residues 175–185 of fibrolase and residues 238–248 of the collagenases (see Table II and Ref. 11). The role of the conserved Phe is unclear, yet it does reinforce the similarities between fibrolase and other zinc-containing metalloproteases such as the collagenases. While this analysis does not delineate the entire metal binding site, it does indicate its position on the polypeptide chain and suggests that two of the ligands are His^{143} and His^{147}. Most likely, the catalytic mechanism utilizes Glu^{144}, as in other zinc proteases (29), although it cannot be ruled out as an additional ligand for zinc.

Numerous algorithms for predicting secondary structure, given the sequence of a protein, are available. One of the most compelling is the method of Cid *et al.* (15), which uses hydrophobicity and solvent accessibility as parameters for assigning structural motifs. Other methods use a probability scheme based upon the structures of proteins which have been determined crystallographically. Examination of the solvent accessibility plot for residues 130–160 shows a pattern of alternating pair of residues (Fig. 10), indicating the formation of an α helix (15). This pattern is more difficult to detect in the hydrophobicity plot (Fig. 9). A helix wheel diagram (Fig. 11) shows that His^{143} and His^{147} would be on the same side of an α helix and would be properly positioned to coordinate to a zinc ion. Other homologous zinc binding sites have been also predicted to helical in structure (18–20). Other methods, such as those of Chou and Fasman (16) and Garnier *et al.* (17), also predict this section to be α helical.

Having the ligands on an α helix would be consistent with the loss of significant helical structure upon addition of EDTA and DTT. In addition, the helix appears to be an amphiphilic structure (hydrophobic moment = 0.11) (see Fig. 11). Amphiphilic helices have been found in numerous protein and peptide systems and can be grouped into several

classes (30,31). Those found in globular proteins appear to have well-defined characteristics. The helix in fibrolase is consistent with those found in other globular proteins, such as having a relatively small hydrophobic moment (the average for other globular proteins is 0.13), a large polar face (≥180°), and a low proportion of charged residues.

SUMMARY

The stability of fibrolase is dependent on the ability to bind the intrinsic zinc atom. Removal of the zinc leads to rapid inactivation of fibrolase. The metal is lost upon exposure to elevated temperatures, acidic pH (pH 5), and addition of metal chelating agents. The zinc binding site has been tentatively identified through sequence homology with other metalloenzymes and through secondary structure analysis. The binding site is predicted to be α helical in structure and loss of zinc has been found to reduce the helix content greatly as determined by CD spectroscopy.

ACKNOWLEDGMENTS

We wish to thank the General Research Fund of the University of Kansas for their support of this project, SmithKline for a grant to purchase the CD spectrophotometer, Dr. Frank Markland for supplying fibrolase, and Dr. Keith Wilkinson for information on the activity assay using the insulin B-chain substrate. We would also like to thank Drs. Robert and A-Young Woody of Colorado State University for providing access to sequence analysis software.

REFERENCES

1. A. Randolph, S. H. Chamberlain, H.-L. C. Chu, A. D. Retzios, F. S. Markland, Jr., and F. R. Masiarz. Amino acid sequence of fibrolase, a direct-acting fibrinolytic enzyme from *Agkistrodon c. contorttrix* venom. *Protein Sci.* (1992), in press.
2. N. K. Ahmed, K. D. Tennant, F. S. Markland, and J. P. Lacz. Biochemical characteristics of fibrolase, a fibrinolytic protease from snake venom. *Haemostasis* 20:147–154 (1990).
3. D. Pretzer, B. Schulteis, C. Smith, D. G. Vander Velde, J. W. Mitchell, and M. C. Manning. Fibrolase, a fibrinolytic protein from snake venom. In Y. J. Wang and R. Pearlman (eds.), *Pharmaceutical Biotechnology, Vol. 5*, Plenum Press, New York (1992), in press.
4. F. S. Markland, K. N. N. Reddy, and L. Guan. Purification and characterization of a direct-acting fibrinolytic enzyme from Southern copperhead venom. In H. Pirkle and F. S. Markland (eds.), *Hemostasis and Animal Venoms*, Marcel Dekker, New York, 1988, pp. 173–189.
5. D. Pretzer, B. S. Schulteis, C. D. Smith, D. G. Vander Velde, J. W. Mitchell, and M. C. Manning. Stability of the thrombolytic protein fibrolase. Effect of temperature and pH on activity and conformation. *Pharm. Res.* 8:1103–1112 (1991).
6. J. Charney and R. M. Tomarelli. A colorimetric method for the determination of the proteolytic activity of duodenal juice. *J. Biol. Chem.* 171:501–505 (1947).
7. D. Eisenberg. Three-dimensional structure of membrane and surface proteins. *Annu. Rev. Biochem.* 53:595–623 (1984).
8. D. Eisenberg, R. M. Weiss, and T. C. Terwilliger. The helical hydrophobic moment: A measure of the amphiphilicity of a helix. *Nature* 299:371–374 (1982).
9. J. Miller, A. D. McLachlan, and A. Klug. Repetitive zinc-binding domains in the protein transcription factor IIIA from *Xenopus* oocytes. *EMBO J* 4:1609–1614 (1985).
10. J. B. Bjarnason and A. T. Tu. Proteolytic specificity and cobalt exchange of hemorrhagic toxin e, a zinc protease isolated from the venom of the Western diamondback rattlesnake (*Crotalus atrox*). *Biochemistry* 22:3370–3374 (1983).
11. B. L. Vallee and D. S. Auld. Zinc coordination, function, and structure of zinc enzymes and other proteins. *Biochemistry* 29:5647–5659 (1990).
12. C. V. Jongeneel, J. Bouvier, and A. Bairoch. A unique signature identifies a family of zinc-dependent metallopeptidases. *FEBS Lett.* 242:211–214 (1989).
13. C. T. Chang, C.-S. C. Wu, and J. T. Yang. Circular dichroic analysis of protein conformation: Inclusion of beta turns. *Anal. Biochem.* 91:13–31 (1978).
14. A. J. Park, L. M. Matrisian, A. F. Kells, R. Pearson, Z. Yuan, and M. Navre. Mutational analysis of the transin (rat stromelysin) autoinhibitor region demonstrates a role for residues surrounding the "cyseine switch." *J. Biol. Chem.* 266:1584–1590 (1991).
15. H. Cid, M. Bunster, E. Arrigada, and M. Campos. Prediction of secondary structure of proteins by means of hydrophobicity profiles. *FEBS Lett.* 150:247–252 (1982).
16. P. Y. Chou and G. D. Fasman. Empirical predictions of protein conformation. *Annu. Rev. Biochem.* 47:251–276 (1978).
17. J. Garnier, D. J. Osguthorpe, and B. Robson. Analysis of the accuracy and implication of simple methods for predicting the secondary structure of globular proteins. *J. Mol. Biol.* 120:97–120 (1978).
18. J. D. Shannon, E. N. Baramova, J. B. Bjarnason, and J. W. Fox. Amino acid sequence of a *Crotalus atrox* venom metalloproteinase which cleaves type IV collagen and gelatin. *J. Biol. Chem.* 264:11575–11583 (1989).
19. J. B. Bjarnason and A. T. Tu. Hemorrhagic toxins from Western diamondback rattlesnake (*Crotalus atrox*) venom: Isolation and characterization of five toxins and the role of zinc in hemorrhagic toxin e. *Biochemistry* 17:3396–3404 (1978).
20. T. Nikai, H. Ishizaki, A. T. Tu, and H. Sugihara. Presence of zinc in proteolytic hemorrhagic toxin isolated from *Agkistrodon acutus* venom. *Comp. Biochem. Physiol.* 72C:103–106 (1982).
21. M. R. Ghadiri and C. Choi. Secondary structure nucleation in peptides. Transition metal ion stabilized alpha helices. *J. Am. Chem. Soc.* 112:1630–1632 (1990).
22. M. R. Ghadiri and A. K. Fernholz. Peptide architecture. Design of stable alpha-helical metallopeptides via a novel exchange-inert Ru(III) complex. *J. Am. Chem. Soc.* 112:9633–9635 (1990).
23. F. Ruan, Y. Chen, and P. B. Hopkins. Metal ion enhanced helicity in synthetic peptides containing unnatural metal-ligating residues. *J. Am. Chem. Soc.* 112:9403–9404 (1990).
24. W. DeW. Horrocks, Jr., J. N. Ishley, B. Holmquist, and J. S. Thompson. Structural and electronic mimics of the active site of cobalt(II)-substituted zinc metalloenzymes. *J. Inorg. Biochem.* 12:131–141 (1980).
25. B. Thomas and A. Wollmer. Cobalt probing of structural alternatives for insulin in solution. *Biol. Chem. Hoppe-Seyler* 370:1235–1244 (1989).
26. J. Baum, C. M. Dobson, P. A. Evans, and C. Hanley. Characterization of a partly unfolded protein by NMR methods: Studies on the molten globule state of guinea pig alpha-lactalbumin. *Biochemistry* 28:7–13 (1989).
27. Y. Goto and A. L. Fink. Conformational states of β-lactamase: Molten-globule states at acidic and alkaline pH with high salt. *Biochemistry* 28:945–952 (1989).
28. T. M. Przybycien and J. E. Bailey. Secondary structure perturbations in salt-induced protein precipitates. *Biochim. Biophys. Acta* 1076:103–111 (1991).
29. D. G. Hanguer, A. F. Monzingo, and B. W. Mathews. An interactive computer graphics study of thermolysin-catalyzed peptide cleavage and inhibition by N-carboxymethyl dipeptides. *Biochemistry* 23:5730–5741 (1984).
30. J. P. Segrest, H. De Loof, J. G. Dohlman, C. G. Brouilette, and G. M. Anantharamaiah. Amphipathic helix motif: Classes and properties. *Proteins Struct. Funct. Genet.* 8:103–117 (1990).
31. J. G. Dohlman, H. De Loof, M. Prabhakaran, W. J. Koopman, and J. P. Segrest. Identification of peptide hormones of the amphipathic helix class using the helical hydrophobic moment algorithm. *Proteins Struct. Funct. Genet.* 6:61–69 (1989).